Proposal for J-PARC 50 GeV Proton Synchrotron

Exclusive Study on the ΛN Weak Interaction in A=4 Λ-Hypernuclei

(Revised from P10 "Study on Λ-Hypernuclei with the Charge-Exchange Reactions")

S. Ajimura, A. Sakaguchi[1], T. Kishimoto,
Osaka University, Toyonaka, Osaka 560-0043, Japan

H. Noumi, T. Takahashi,
High Energy Accelerator Research Organization (KEK), Tsukuba, Ibaraki 305-0801, Japan

T. Fukuda, Y. Mizoi,
Osaka Electro-communications University, Neyagawa, Osaka 572-8530, Japan

M. Iio, H. Ohnishi, H. Outa,
Institute of Physical and Chemical Research (RIKEN), Wako, Saitama 351-0198, Japan

H. Bhang,
Seoul National University, Seoul 151-742, Korea

P.K. Saha,
Japan Atomic energy Agency (JAEA), Tokai, Ibaraki 319-1195, Japan

L. Busso,
Università di Torino, I-10125 Torino, Italy

D. Faso,
INFN, Sezione di Torino, I-10125 Torino, Italy

and

O. Morra
INAF-IFSI, Sezione di Torino, C.so Fiume 4, I-10125 Torino, Italy

10 December, 2006

Abstract

We propose to study the ΛN weak interaction by measuring the non-mesonic weak decay (NMWD) of Λ-hypernuclei. The ΛN NMWD process, $\Lambda N \rightarrow NN$, happens only in the Λ-hypernuclei and important information on the baryon-baryon weak interaction can be obtained. Light hypernuclei, such as ${}^{4}_{\Lambda}$H, ${}^{4}_{\Lambda}$He and ${}^{5}_{\Lambda}$He, are the best hypernuclei to study the spin, isospin and parity structures of the baryon-baryon weak interaction, but experimental information is quite scarce. We propose a precise measurement of the NMWD process of the ${}^{4}_{\Lambda}$He hypernucleus as a Day-1 experiment.

[1]Spokesperson, e-mail: sakaguch@phys.sci.osaka-u.ac.jp, phone: +81-6-6850-5352.

1 Changes from the previous proposal (P10)

In the previous proposal, P10 "Study on Λ-Hypernuclei with the Charge-Exchange Reactions", we proposed to carry out a series of experiments by using single- and double-charge exchange reactions. The subjects of the experiments were the production of neutron-rich hypernuclei and the detailed studies on the ΛN weak interaction. Although the subjects had a weak coupling each other in concepts of physics, both studies required a high intensity beamline in the ultimate goal, and we arranged the experiments in one proposal. On the previous proposal, PAC pointed out "*the lack of a unique installation for the whole series of measurements*" and requested "*a more detailed scheduling of the activities*".

Following the comments from PAC, we decided to update the previous proposal as two separated experimental proposals to respond to the comments clearly and unambiguously. In this proposal, we discuss on the experiments to investigate the ΛN weak interaction by measurements of the non-mesonic weak decay (NMWD) in the A=4 Λ-hypernuclei. Current status and prospects of studies on the ΛN weak interaction were revised. The details of the experimental procedures, detector performance simulations and cost estimations were updated.

2 Introduction

The Λ-hypernucleus was identified experimentally for the first time in 1953 in a nuclear emulsion exposed to cosmic rays[1]. Since then, number of experiments have been carried out, innovative methods/techniques have been developed and many aspects of the Λ-hypernuclei have become clear.

Studies on the Λ-hypernuclei in the past were categorized mainly in two subjects. One was the study of the Λ-hypernuclei as another nuclei with the strangeness degrees of freedom. Precise measurements of level structures of the Λ-hypernuclei made it possible to study the hyperon-nucleon strong interaction. Another subject was the study on the ΛN weak interactions. As well know, the Λ hyperon decays to a pion and a nucleon by the weak interaction in the free space, $\Lambda \rightarrow N\pi$. Similar decay mode exists in the Λ-hypernuclei known as the mesonic weak decay (MWD). Since the momentum of the decay nucleon from the MWD process is about 100 MeV/c which is smaller than the Fermi momentum of nucleons in nuclei, the MWD process is suppressed strongly in heavy hypernuclei due to the Pauli blocking. Another decay mode, so called non-mesonic weak decay (NMWD) mode, in which a Λ hyperon and a nucleon goes to two nucleons (ΛN→NN), is possible in the Λ-hypernuclei. The decay momentum of the NMWD process is about 400 MeV/c and the decay nucleons are almost free from the Pauli blocking. The new decay mode provides a powerful tool to study the baryon-baryon weak interaction, for which experimental studies are usually quite difficult.

In this proposal, we propose to study the ΛN weak interaction by the measurements of NMWD for A=4 Λ-hypernuclei.

2.1 Study on ΛN weak interaction

The study on the weak ΛN interaction has long history experimentally and theoretically. In recent years, precise measurements of branching ratios, total decay widths and decay asymmetries became available from a series of experiments, and estimated values for these observables from different theoretical calculations were converged. However, explanations of the experimental values by the theoretical calculations are still controversial. The situation is described in the following sections.

Table 1: Six amplitudes in the non-mesonic weak decay process whose initial ΛN system is in relative S-states.

Initial	Final	Matrix element	Rate	I_f	Parity change
$^1S_0$	$^1S_0$	a	a^2	1	no
	$^3P_0$	$\frac{b}{2}(\sigma_1-\sigma_2)q$	b^2	1	yes
$^3S_1$	$^3S_1$	c	c^2	0	no
	$^3D_1$	$\frac{d}{2\sqrt{2}}S_{12}(q)$	d^2	0	no
	$^1P_1$	$\frac{\sqrt{3}}{2}e(\sigma_1-\sigma_2)q$	e^2	0	yes
	$^3P_1$	$\frac{\sqrt{6}}{4}f(\sigma_1+\sigma_2)q$	f^2	1	yes

Another long standing puzzle is the dominance of the ΔI=1/2 channel over the ΔI=3/2 channel, so called "ΔI=1/2 rule", which is necessary to explain the kaon and hyperon weak decays but it is difficult to reproduce with theoretical calculations. There are discussions that the "ΔI=1/2 rule" may be broken in NMWD of Λ-hypernuclei, but conclusion is not obtained, yet. Since the decay momentum of the NMWD process, about 400 MeV/c, is considerably high, the baryon-baryon weak interaction in a short distance becomes important. Such short-range interaction may be described by a quark-exchange model which predicts a strong ΔI=3/2 contribution[2].

2.1.1 Partial decay rates of non-mesonic weak decay

The matrix element of the non-mesonic weak decay can be classified into six amplitudes depending on the spin, isospin and parity of the initial and final states as shown in Table 1 provided that the initial state is of relative S-wave[3]. The study of partial decay rates, $\Gamma(\Lambda n \to nn) \equiv \Gamma_n$ and $\Gamma(\Lambda p \to np) \equiv \Gamma_p$, can constrain magnitude of each amplitude in terms of isospin (I_f in Table 1) because the nn system is in a pure isospin 1 state and the np system is a mixture of the isospin 1 and 0 states. A phenomenological analysis of s-shell hypernuclei predicted the dominance of the I_f=1 amplitude (amplitude f) from the ${}^{4}_{\Lambda}$H and ${}^{4}_{\Lambda}$He NMWD data[3]. The prediction was supported experimentally because Γ_n/Γ_p ratios, so-called np-ratios, close to unity were observed for the ${}^{5}_{\Lambda}$He and ${}^{12}_{\Lambda}$C hypernuclei[4, 5]. On the contrary, theoretical estimations based on the pion exchange model implied the dominance of the I_f=0 amplitudes (amplitudes c and d) which was reflecting the strong tensor interaction due to π-meson exchange[6, 7], and predicted vanishing branching ratios to the I_f=1 channels. This discrepancy had existed for a long time even though heavier mesons, like ρ/ω, K/K* and σ, were included in the calculations[8, 9].

Recently KEK-PS-E462[10] and E508[11] experiments have been carried out in order to solve the discrepancy. In the experiments, all the decay particles (np and nn pairs) from the $\Lambda N \to NN$ process were measured and the kinematics of the non-mesonic weak decay, a back-to-back emission of a NN pair, were reconstructed, in order to avoid the contribution due to the final state interaction and the $\Lambda NN \to NNN$ three body process[12, 13]. If the $\Lambda N \to NN$ process happens from a ΛN pair at rest, the NN pair in the final state is emitted back-to-back due to the momentum conservation. Although the Λ and N in hypernuclei have the Fermi motion and the back-to-back correlation is smeared, the angular correlation still remains and can be seen clearly experimentally. The NN angular correlation was demonstrated in Ref.[14] for the first time in the $\Lambda p \to np$ decay (see Fig.1 top), and was clearly seen for both NMWD channels, $\Lambda p \to np$ and $\Lambda n \to nn$, in the E462 experiment[15] (see Fig.1 bottom).

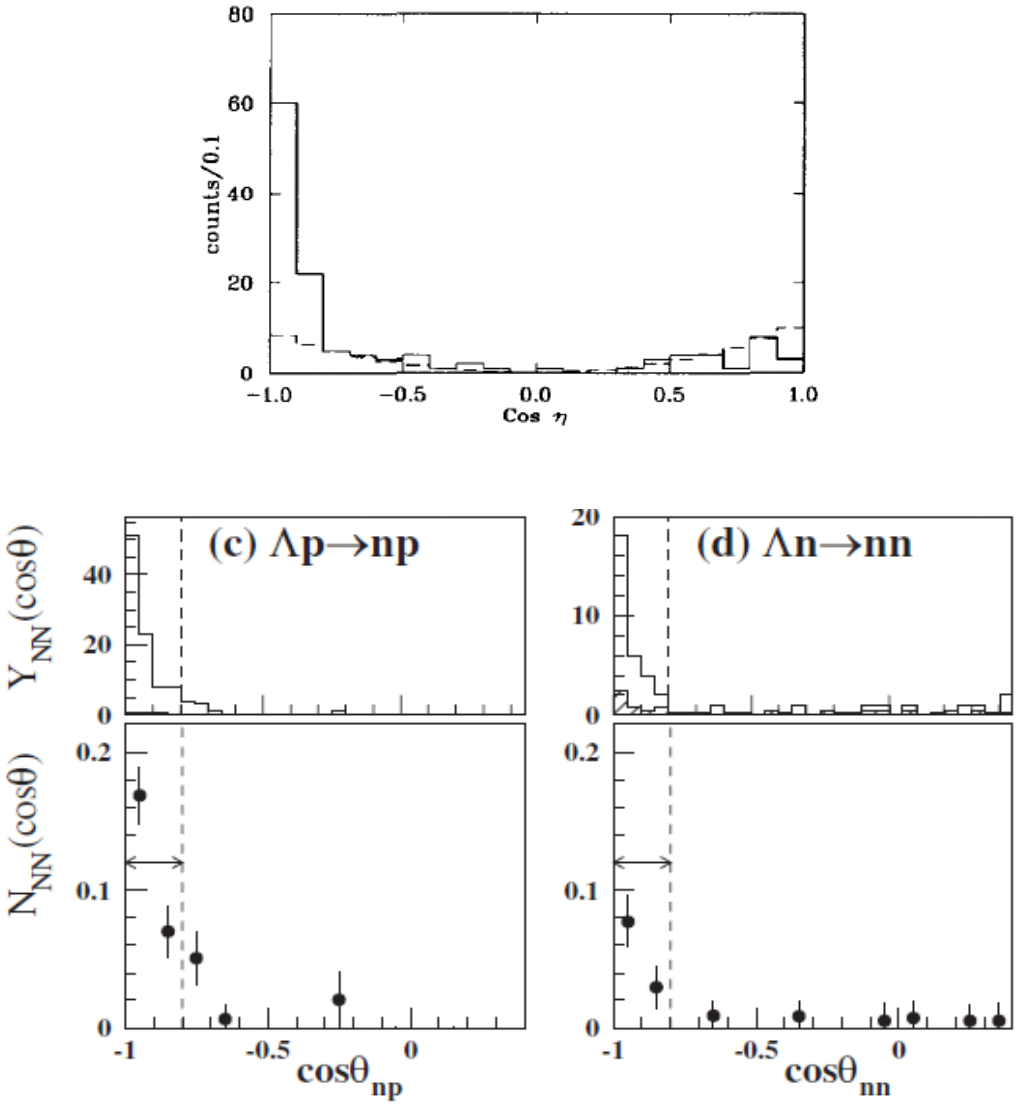

Figure 1: (Top) Angular correlation between np pairs from NMWD of the ${}^{4}_{\Lambda}$He hypernucleus reported in Ref.[14]. Horizontal axis corresponds to cos of the opening angle of np, and one can see clear enhancement at Cos η=$-$1. (Bottom) Angular correlation between np (left) and nn (right) pairs from NMWD of the ${}^{5}_{\Lambda}$He hypernucleus shown in Ref.[15]. Horizontal axis corresponds to cos of the opening angle of the two nucleons, and one can see clear enhancement at $\cos\theta_{np,nn}$=$-$1.

Table 2: Summary of results of the Γ_n/Γ_p ratio measurements in the past.

	old	ref.	recent	ref.
${}^{12}_{\Lambda}$C	$1.33^{+1.12}_{-0.81}$	[4]	$0.51 \pm 0.13 \pm 0.04$	[17]
	$1.87 \pm 0.59^{+0.32}_{-1.00}$	[5]		
${}^{5}_{\Lambda}$He	$0.77 \rightarrow 2.0$	[18]	$0.45 \pm 0.11 \pm 0.03$	[15]
	≥ 1.4	[19]		
	0.87 ± 0.37	[4]		
${}^{4}_{\Lambda}$He	$0.43^{+0.24}_{-0.18}$	[20]	n.a.	
	$0.67^{+0.19}_{-0.15}$	[21]		
	$0.06^{+0.28}_{-0.06}$	[22]		
	0.25 ± 0.13	[14]		
${}^{4}_{\Lambda}$H	n.a.		n.a.	

The Γ_n/Γ_p ratios were obtained from the new KEK-PS experiments[15, 16, 17]. The values were:

$$0.45 \pm 0.11(stat) \pm 0.03(syst) \qquad \text{for } {}^{5}_{\Lambda}\text{He}$$

$$0.51 \pm 0.13(stat) \pm 0.04(syst) \qquad \text{for } {}^{12}_{\Lambda}\text{C}.$$

The new results were different from that of old measurements in which the ratios were larger than or close to unity. It indicated that the I_f=1 component was not negligible as previous experiments had been pointed out but the amplitude was smaller than the I_f=0 component. Table 2 is a summary of the results of the Γ_n/Γ_p ratio for light hypernuclei in the past. The experiments also told us the importance of the effects due to the final state interaction and/or the $\Lambda NN \rightarrow NNN$ three body process. The E462 experiment found that the effect was about 30% of the non-mesonic weak decay even for the light hypernucleus ${}^{5}_{\Lambda}$He. Therefore, the exclusive measurement with coincidence of all the decay particles is essential to determine the observables of NMWD.

On the other hand, the most recent theoretical calculations showed that the pion and the kaon exchanges contributed constructively to the I_f=1 amplitude f, which had been vanishing in the old calculations, and destructively to the I_f=0 amplitudes c and d, which had been dominant over the $I_f = 1$ amplitudes. The new theoretical partial decay rates are now compatible with the recent experimental results, consequently[23, 24, 25].

2.1.2 Weak decay of spin polarized Λ-hypernuclei

The parity violation of the NMWD process provides us interesting quantity to investigate the spin and parity structures of the ΛN weak interaction. The quantity is the decay asymmetry parameter, which relates to the asymmetric emission of decay particle with respect to the Λ spin polarization[26]. The asymmetry is due to the interference between parity conserving and violating amplitudes, and is expressed in terms of the six amplitudes in Table 1 as follows [27]:

$$\alpha_p^{NM} = \frac{2\sqrt{3}Re[-ae^* + b(c - \sqrt{2}d)^*/\sqrt{3} - f(\sqrt{2}c + d)^*]}{\{a^2 + b^2 + 3(c^2 + d^2 + e^2 + f^2)\}}. \tag{1}$$

As discussed in the previous section, the amplitudes c, d and f are considered to have large contributions to the NMWD widths, theoretically. Therefore, the asymmetry parameter is

mainly determined by the last term in Eq.(1), $f(\sqrt{2}c + d)^*$, which is sensitive to the $^3S_1$ component in the initial ΛN state. However, there are other two terms, ae^* and $b(c - \sqrt{2}d)^*$, which come from the interference between the initial $^1S_0$ and $^3S_1$ amplitudes. These two terms were ignored in the old theoretical expression by Bando, *et al.*[28], since the $^1S_0$ states have no asymmetry by themselves. A calculation based on the direct quark-exchange model suggested the importance of the initial $^1S_0$ state[29]. Therefore, the reason of the importance of the decay asymmetry parameter is that the parameter is sensitive to the both initial states, $^1S_0$ and $^3S_1$, while the decay rates (except for the NMWD of ${}^4_\Lambda$H and ${}^4_\Lambda$He) is not affected so much by the $^1S_0$ initial state because each amplitude is weighted by the spin factor, $2S + 1$, in the expression of the partial decay rates ($2S + 1$=3 for the $^3S_1$ states and $2S + 1$=1 for $^1S_0$).

Experimentally, a quite large value, α_p^{NM}=−1.3 ± 0.4, of the asymmetry parameter was observed for NMWD of the polarized ${}^{12}_\Lambda$C and ${}^{11}_\Lambda$B hypernuclei by using the ^{12}C(π^+, K^+) reaction in the KEK-PS-E160 experiment[30]. It suggested an equal importance of the I_f=0 (c and d) and I_f=1 (f) amplitudes and seemed to contradict the phenomenological analysis of branching ratios at that moment, which suggested the dominance of the I_f=1 state. However, we had an error of 40% for the asymmetry parameter. It was far below the accuracy that was needed for the detailed comparison with theoretical calculations. We thus have carried out a new experiment where the asymmetric non-mesonic weak decay was observed from the decay of a polarized ${}^5_\Lambda$He hypernucleus[31].

The E278 experiment was carried out at the K6 beamline of KEK-PS. The ^{6}Li$(\pi^+, K^+p)^5_\Lambda$He reaction at P_π=1.05GeV/c was used to produce the polarized ${}^5_\Lambda$He. The experiment demonstrated that the polarized ${}^5_\Lambda$He hypernucleus was really produced by the (π^+, K^+) reaction[32]. The degrees of the polarization was determined experimentally from the decay asymmetry of the mesonic weak decay of the hypernucleus. The large asymmetry parameter and the large π^- branching ratio of the ${}^5_\Lambda$He MWD were essential for the precise measurement of the degrees of the polarization of the Λ-hyperon in the hypernucleus. The observed polarization was consistent with the DWIA calculation[33], which included the Λ polarization in the elementary reaction, ^{6}Li$(\pi^+, K^+)^6_\Lambda$Li, and the depolarization due to the proton emission, ${}^6_\Lambda$Li→${}^5_\Lambda$He+p.

The asymmetry parameter of NMWD derived from the Λ polarization and the proton decay asymmetry was [34]:

$$\alpha_p^{NM} = 0.24 \pm 0.22 \qquad \text{for } {}^5_\Lambda\text{He (E278)}.$$

The result showed that the asymmetry parameter of NMWD had a positive sign and its magnitude was quite small compared with that obtained in the E160 experiment. One expected a contribution of the relative P-state in the initial ΛN system for the p-shell hypernuclei, ${}^{12}_\Lambda$C and ${}^{11}_\Lambda$B, although most of the decay rate came from the initial S-state according to Ref.[35]. The theoretical calculations based on the meson-exchange model estimated the asymmetry parameter to be around -0.7 independently of hypernuclear species. So, the theory preferred the results of the E160 experiment rather than the E278 experiment.

Recently, the KEK-PS-E462 experiment has been carried out by using the same reaction as the E278 experiment. The result suggested that the asymmetry parameter of the non-mesonic weak decay of the ${}^5_\Lambda$He hypernucleus was[36]:

$$\alpha_p^{NM} = 0.08 \pm 0.08^{+0.08}_{-0.00} \qquad \text{for } {}^5_\Lambda\text{He (E462)}.$$

which was quite small and consistent with the E278 experiment (see also Fig.2). Besides, a preliminary analysis of the KEK-PS-E508 experiment showed that the asymmetry parameters for NMWD of the ${}^{12}_\Lambda$C and ${}^{11}_\Lambda$B hypernuclei are also as small as that of the ${}^5_\Lambda$He case, and contradicts the E160 result. Although, the definite conclusion can not be derived from the E508 experiment due to the difficulty in the determination of the hypernuclear polarization,

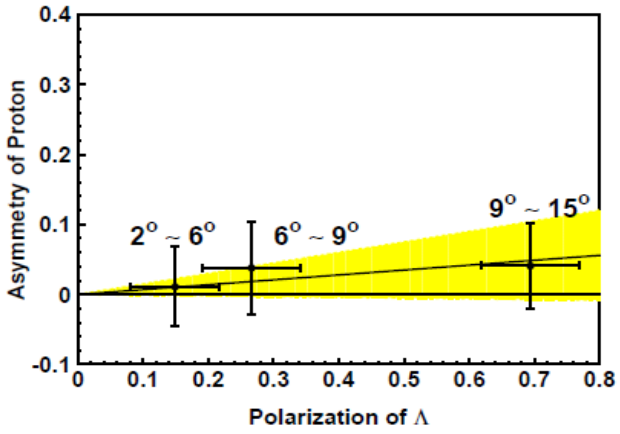

Figure 2: The plot shows the proton decay asymmetry of NMWD vs the polarization of a Λ-hyperon in ${}^{5}_{\Lambda}$He. The tangent of the correlation between the proton asymmetry and the Λ polarization is a measure of the decay asymmetry parameter.

Table 3: Allowed spin states of the initial ΛN pair in the A=4 and 5 hypernuclei.

Hypernucleus	$\Lambda n \rightarrow nn$	$\Lambda p \rightarrow np$
${}^{4}_{\Lambda}$H	${}^{1}S_0$, ${}^{3}S_1$	${}^{1}S_0$
${}^{4}_{\Lambda}$He	${}^{1}S_0$	${}^{1}S_0$, ${}^{3}S_1$
${}^{5}_{\Lambda}$He	${}^{1}S_0$, ${}^{3}S_1$	${}^{1}S_0$, ${}^{3}S_1$

the experiments suggest the asymmetry parameter for NMWD is small also for the p-shell hypernuclei.

So, currently we believe the values of the asymmetry parameter of NMWD are small, close to 0, for both s- and p-shell Λ-hypernuclei, while the theory estimates it to be around -0.7.

2.1.3 Importance of precise measurements of A=4 and 5 hypernuclei

As discussed above, recent experimental results on the branching ratios became compatible with the theoretical estimations. However, most of theoretical calculations could not explain the values of the asymmetry parameter. Several theoretical attempts were carried out to override the situation by introducing a σ meson exchange together with a quite strong breaking of the ΔI=1/2 rule[37] or by introducing an exchange of a very heavy meson[38], but the justification of such modifications in theories were necessary.

As we mentioned, the branching ratios (or partial decay rates) are mainly determined by the initial ${}^{3}S_1$ amplitudes because the spin factor, $2S+1$, of the initial ${}^{3}S_1$ states are three times larger than that of the ${}^{1}S_0$ states. However, the asymmetry parameter is determined by the interference not only among the initial ${}^{3}S_1$ states but also between the initial ${}^{3}S_1$ and ${}^{1}S_0$ states. Therefore the exclusive measurement of the initial ${}^{1}S_0$ contribution is essential to understand the branching ratio and the decay asymmetry of NMWD at the same time. Table 3 shows allowed initial states of NMWD in the $\Lambda n \rightarrow nn$ and $\Lambda p \rightarrow np$ channels for the A=4 and 5 hypernuclei. Since a pp (nn) pair in ${}^{4}_{\Lambda}$He (${}^{4}_{\Lambda}$H) forms 0^+ state, and Λ and n (p) couples to 0^+ to form overall 0^+ spin-parity of the hypernuclear ground state, then the $\Lambda n \rightarrow nn$ ($\Lambda p \rightarrow np$) decay for the ${}^{4}_{\Lambda}$He (${}^{4}_{\Lambda}$H) hypernucleus starts only from the ${}^{1}S_0$ states. So, one can determine

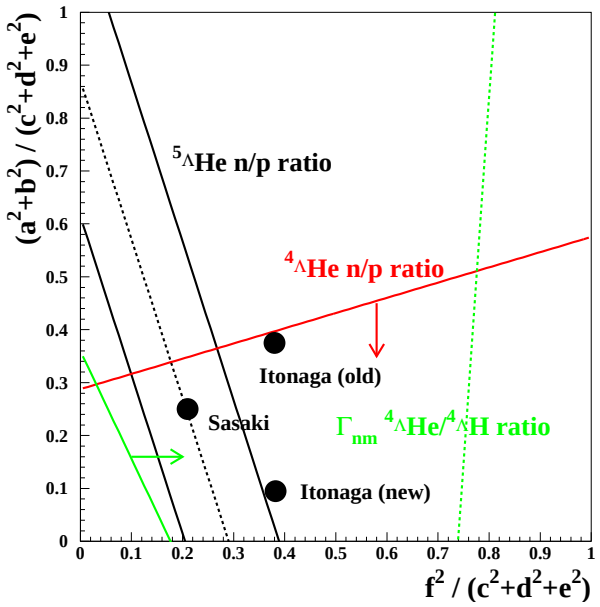

Figure 3: Allowed region of the NMWD amplitudes from a model-independent analysis with the NMWD data of A=4 and 5 hypernuclei. Solid circles are predictions from theoretical calculations. See text for more details.

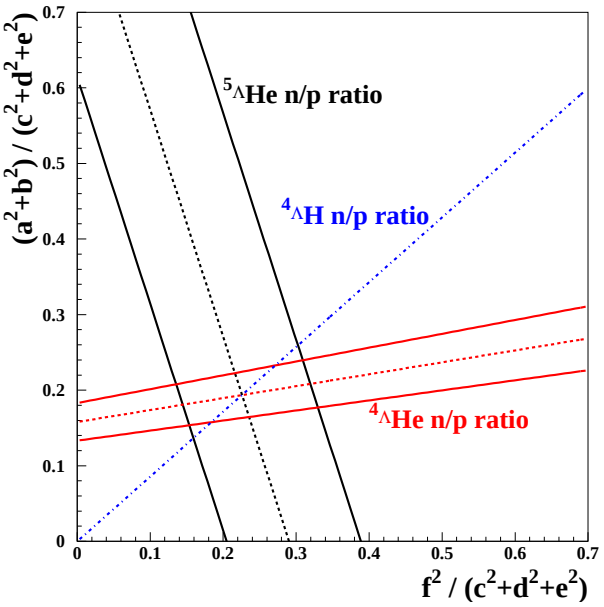

Figure 4: Prospects of the determination of the NMWD amplitudes if we measure the $\Gamma_n/\Gamma_p(^4_\Lambda\mathrm{He})$ ratio with a 15% accuracy (red lines). The blue line is a demonstration how the $\Gamma_n/\Gamma_p(^4_\Lambda\mathrm{H})$ ratio constrains the amplitudes.

the initial $^1S_0$ amplitude directly with measurements of these decay modes.

Figure 3 shows allowed regions of the NMWD amplitudes from a simple model-independent analysis with the NMWD data of A=4 and 5 hypernuclei by assuming the ΔI=1/2 rule. The horizontal and vertical axes are the ratios $f^2/(c^2+d^2+e^2)$ and $(a^2+b^2)/(c^2+d^2+e^2)$, respectively. The black, red and green solid lines indicate 1σ boundary of the regions from the experimental $\Gamma_n/\Gamma_p(^5_\Lambda\mathrm{He})$, $\Gamma_n/\Gamma_p(^4_\Lambda\mathrm{He})$ and $\Gamma_{nm}(^4_\Lambda\mathrm{He})/\Gamma_{nm}(^4_\Lambda\mathrm{H})$ ratios, respectively[15, 22, 14]. We used following equations in the model-independent analysis:

$$\frac{\Gamma_n}{\Gamma_p}(^5_\Lambda\mathrm{He}) = \frac{3R_{n1}+R_{n0}}{3R_{p1}+R_{p0}}, \qquad \frac{\Gamma_n}{\Gamma_p}(^4_\Lambda\mathrm{He}) = \frac{2R_{n0}}{3R_{p1}+R_{p0}}, \qquad \frac{\Gamma_{nm}(^4_\Lambda\mathrm{He})}{\Gamma_{nm}(^4_\Lambda\mathrm{H})} = \frac{3R_{p1}+R_{p0}+2R_{n0}}{3R_{n1}+R_{n0}+2R_{p0}}$$

$$R_{p1} = c^2+d^2+e^2+f^2, \qquad R_{p0} = a^2+b^2$$
$$R_{n1} = \kappa_f f^2, \qquad R_{n0} = \kappa_{ab}(a^2+b^2), \qquad \kappa_f = \kappa_{ab} = 2.$$

Currently, the NMWD amplitudes are strongly restricted only by the $\Gamma_n/\Gamma_p(^5_\Lambda\mathrm{He})$ ratio, and the well restricted $f^2/(c^2+d^2+e^2)$ ratio is a ratio of amplitudes within the $^3S_1$ component. The ratio $(a^2+b^2)/(c^2+d^2+e^2)$, which is a ratio between the $^1S_0$ and $^3S_1$ amplitudes, is poorly determined. Solid circles show several theoretical predictions[25, 38, 39]. It is clear that we need more accurate experimental information on the $^4_\Lambda$He and $^4_\Lambda$H hypernuclei to pin down the NMWD amplitudes. Figure 4 shows prospects of the amplitude determination if we measure the $\Gamma_n/\Gamma_p(^4_\Lambda\mathrm{He})$ ratio with a 15% acculacy (red lines). The measurement may improve the situation of the amplitude determination dramatically.

The measurement of the asymmetry parameter for $^5_\Lambda$He is also important, since we can not determine each amplitude of a specific initial state only from the measurement of the partial

decay rate. Before the E462 experiment, only the decay protons were measured to derive the asymmetry parameter. As mentioned above, the effect of the final state interaction was considerably large even for ${}^{5}_{\Lambda}$He. Recently, E462 reported the asymmetry parameter of ${}^{5}_{\Lambda}$He by a coincidence measurement of a pair of proton and neutron in the back-to-back kinematics[36]:

$$\alpha_p^{NM} = 0.31 \pm 0.22.$$

So, we already have an accurate information on the decay amplitudes from the asymmetry measurement which is complementary with the information to be obtained from the study on the A=4 hypernuclei.

2.1.4 Investigation of the ΔI=1/2 rule in NMWD

There is another interest in the measurement of the ${}^1S_0$ amplitudes. Among the amplitudes listed in Table 1, the a, b and f amplitudes are sensitive to the "ΔI=1/2 rule", and the a and b amplitudes or the ${}^1S_0$ amplitudes can be extracted from the NMWD measurements of the A=4 hypernuclei as we mentioned above. If the ΔI=1/2 rule is hold in the non-mesonic weak decay, the ratio of two decay widths, Γ_p of ${}^{4}_{\Lambda}$H and Γ_n of ${}^{4}_{\Lambda}$He, is expected to be 1:2, while if ΔI=3/2 amplitude dominates we will find the ratio to be 2:1.

$$\frac{\Gamma_p({}^{4}_{\Lambda}\mathrm{H})}{\Gamma_n({}^{4}_{\Lambda}\mathrm{He})} = \frac{1}{2} \qquad \text{if } \Delta I = 1/2 \text{ dominant},$$

$$\frac{\Gamma_p({}^{4}_{\Lambda}\mathrm{H})}{\Gamma_n({}^{4}_{\Lambda}\mathrm{He})} = 2 \qquad \text{if } \Delta I = 3/2 \text{ dominant}.$$

The precise measurements of these decay modes can provide an opportunity to test the ΔI=1/2 rule in NMWD. So far, the ΔI=1/2 rule have been proposed from the experimental results of the free weak decays of hyperons and mesons, and the ΔI=3/2 component was believed to be very small in the weak process.

Another test of the contribution of the ΔI=3/2 amplitude in the NMWD process has been discussed by Schumacher[40], in which experimental values of $\Gamma_n/\Gamma_p({}^{4}_{\Lambda}\mathrm{He})$, $\Gamma_n/\Gamma_p({}^{5}_{\Lambda}\mathrm{He})$ and $\Gamma_{nm}({}^{4}_{\Lambda}\mathrm{He})/\Gamma_{nm}({}^{4}_{\Lambda}\mathrm{H})$ have been used. Experimental data on NMWD of the ${}^{4}_{\Lambda}$He and ${}^{4}_{\Lambda}$H hypernuclei are also important for such a test. The blue line in Fig.4 demonstrates how we can constrain the NMWD amplitudes by the measurement of the ratio $\Gamma_n/\Gamma_p({}^{4}_{\Lambda}\mathrm{H})$, which is represented as:

$$\frac{\Gamma_n}{\Gamma_p}({}^{4}_{\Lambda}\mathrm{H}) = \frac{3R_{n1} + R_{n0}}{2R_{p0}}.$$

If the ΔI=1/2 rule holds, the region of the amplitudes determined by the three ratio measurements should have an overlap. If there is no overlap, it strongly suggests the breaking of the ΔI=1/2 rule in NMWD of hypernuclei.

3 Proposed Experiments

As we discussed in the previous section, the measurement of the NMWD process for the A=4 and 5 hypernuclei are quite important and the lack of the experimental information on NMWD of the A=4 hypernuclei prevents us to discuss the details of the ΛN weak interaction. So, new experimental data on the A=4 hypernuclei are awaiting.

Here, we propose studies on the NMWD process of the A=4 hypernuclei. We believe the measurement of NMWD for the ${}^{4}_{\Lambda}$He hypernucleus is possible as a Day-1 experiment, and we will be able to provide an experimental information to pin down the NMWD amplitudes. We wish to emphasize that the information is also important for the discussion of the "ΔI=1/2 rule" in the future. We concentrate on the ${}^{4}_{\Lambda}$He measurement in this proposal, and we discuss the details of the experimental procedure for the measurement in this section.

To discuss the "ΔI=1/2 rule" in NMWD of hypernuclei unambiguously, we have to measure also the decay of the ${}^{4}_{\Lambda}$H hypernucleus. The measurement requires a drastic improvement of experimental techniques, and we think the construction of the High-Intensity and High-Resolution (HIHR) beamline[41] is one of key issues for the improvement. The construction of the HIHR beamline is a long-range plan, and the time scale is out of the scope of this experimental proposal. The experimental procedures for the study on NMWD of ${}^{4}_{\Lambda}$H hypernucleus is described briefly in Appendix A, and the conceptual design of the HIHR beamline is described in Appendix B.

3.1 Precise measurement of NMWD of ${}^{4}_{\Lambda}$He as Day-1 experiment

We propose to measure the NMWD partial decay widths of the ${}^{4}_{\Lambda}$He hypernucleus as a Day-1 experiment at the J-PARC 50 GeV proton synchrotron facility. The precise determination of the partial decay widths, $\Gamma(\Lambda n \rightarrow nn)$ and $\Gamma(\Lambda p \rightarrow np)$, requires a copious production of the ${}^{4}_{\Lambda}$He hypernucleus and an efficient detection of the decay processes. The combination of the K1.8 slow-extraction beamline, Superconducting Kaon Spectrometer (SKS) and a large acceptance decay arm detector system are the best solution for such a study. Once we determine the partial decay widths of ${}^{4}_{\Lambda}$He NMWD, we can set strong constraint to the NMWD decay amplitudes as we discussed in Sec.2.1.3.

3.1.1 K1.8 beamline and SKS spectrometer

We are planning to use the ^{4}He$(\pi^+, K^+){}^{4}_{\Lambda}$He reaction with 1.1 GeV/c π^+ beam from the K1.8 beamline at the J-PARC 50 GeV PS to produce the ${}^{4}_{\Lambda}$He hypernucleus. Figure 5 shows a layout of the primary target, K1.8 beamline and spectrometer in the 50GeV PS experimental facility.

Since the non spin-flip interaction is strong for the (π^+, K^+) reaction at the pion beam momentum, the reaction populates the 0^+ ground states of the ${}^{4}_{\Lambda}$He hypernucleus. Theoretical estimation of the reaction cross section was done based on a DWIA calculation[42], and the cross section is shown in Fig.6 as a function of the pion beam momentum. The pion beam energy dependence of the production cross section of ${}^{4}_{\Lambda}$He(g.s., 0^+) has two plateaus in the regions 1.1–1.2GeV/c and 1.4–1.5GeV/c. By taking into account available large acceptance spectrometers with good momentum resolutions at Day-1 and momentum dependence of the spectrometer resolutions[43], we are planning to use the K1.8 beamline, to be available at Day-1, and set the beamline momentum to 1.1 GeV/c.

The Superconducting Kaon Spectrometer (SKS) is used to detect produced K^+ to achieve a large angular acceptance (∼100 msr) and a good momentum resolution at the same time.

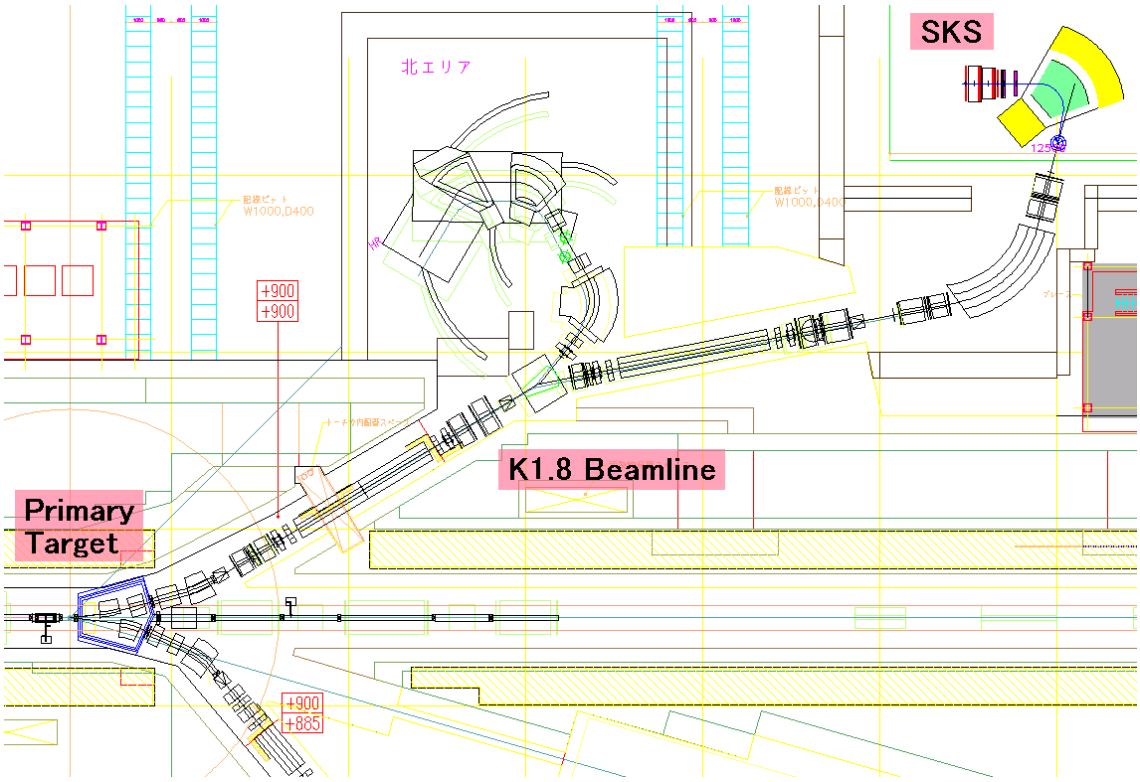

Figure 5: Floor plan of the primary target, K1.8 beamline and SKS spectrometer.

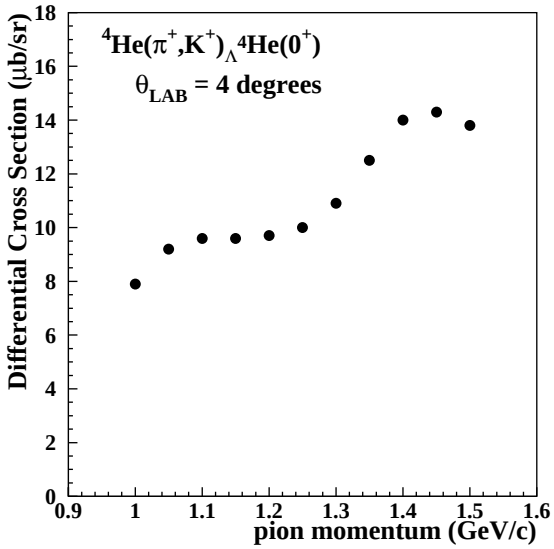

Figure 6: Theoretically estimated differential cross section of the $^4\mathrm{He}(\pi^+, K^+)^4_\Lambda\mathrm{He}$(g.s., 0^+) reaction at θ_{LAB}=4° based on a DWIA calculation[42].

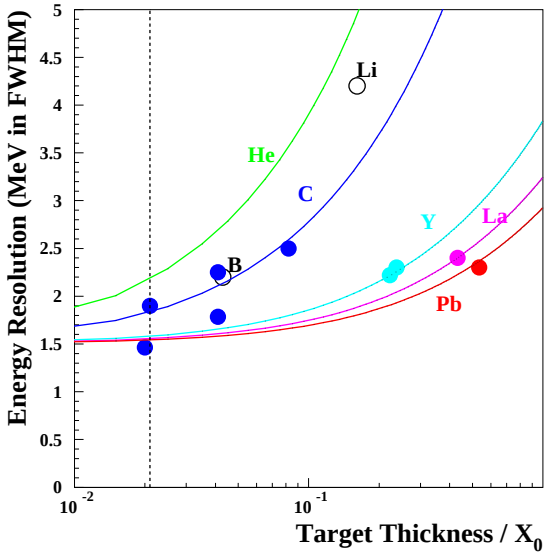

Figure 7: Excitation energy resolutions achieved in the past experiments with SKS as a function of the target thicknesses in a unit of radiation lengths (circles). See text for more details.

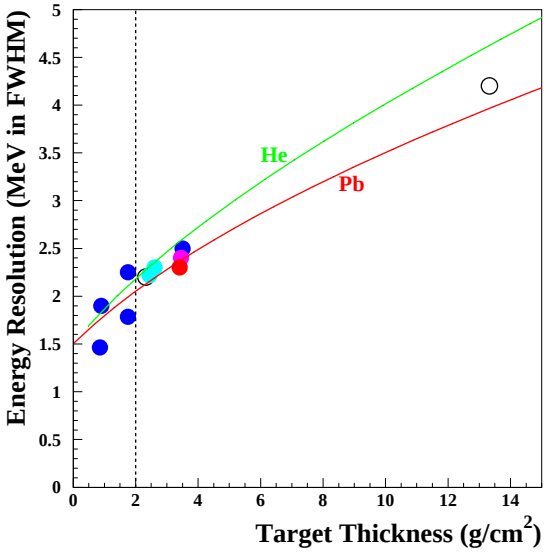

Figure 8: Same plot as Fig.7 with a horizontal axis in a unit of g/cm^2.

The mass (excitation energy) resolution of hypernuclei should be less than 2 MeV (FWHM), since the binding energy of the ground state of ${}^{4}_{\Lambda}$He is 2.42 ± 0.04 MeV[44].

Figures 7 and 8 show summaries of excitation energy resolutions (FWHM) achieved by SKS in past experiments[45, 46, 47, 48, 49] as a function of the target thicknesses in the units of the radiation length (Fig.7) and length in g/cm^2 (Fig.8). The curves in the figures are results of simple estimations of the resolution with energy-loss and multiple-scattering in targets and other contributions (includes intrinsic resolutions of the beamline spectrometer and SKS and the momentum spread due to materials in the beamline). Red, purple, light-blue, blue and green colors correspond to Pb, La, Y, C and He targets, respectively. The energy resolution is dominated by the contribution from the energy-loss straggling in the case of the (π^+, K^+) reaction, which is roughly proportional to the square-root of the target thickness in g/cm^2. For thin targets, other contributions independent from the target thickness are not negligible. Since we are planning to use a liquid He (LHe) target of about 2 g/cm^2 in thickness ($\sim$15cm, $\sim$0.02 X$_0$), we can achieve the required resolution, 2 MeV. Figure 9 shows a result of a simple simulation calculation of the excitation energy (Ex) spectrum with the 2 MeV resolution. The amount of the quasi-free Λ production background was assumed to be 10 times as much as that of the signal ${}^{4}_{\Lambda}$He production in the region Ex$<$15MeV. The yields in the figure corresponds to 4 weeks of beam time.

3.1.2 Decay arm: detection of particles from NMWD

Particles from the weak decay of hypernuclei are measured by the decay arm detector system which consists of a cylindrical drift chamber (CDC) and a stack of plastic scintillation counters (range counter system and TOF counter system) as shown in Figs. 10 and 11.

CDC is for the tracking of the charged particles (protons and charged pions). CDC will be

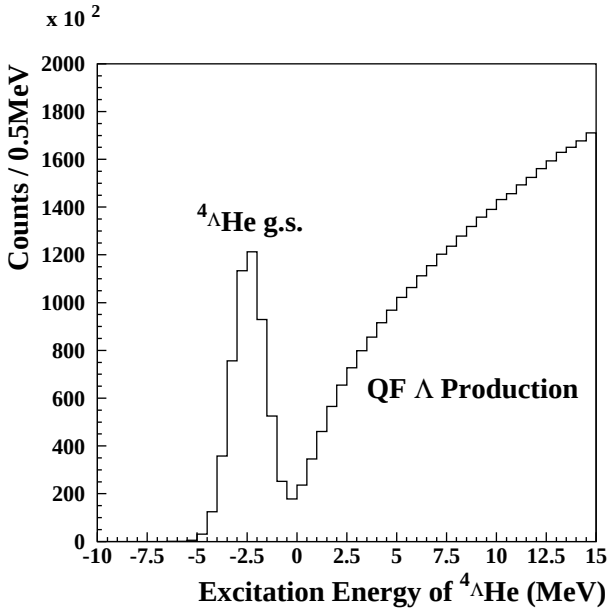

Figure 9: Simulation calculation of the excitation energy spectrum of the ^{4}He(π^+, K^+) reaction. The energy resolution of 2 MeV (FWHM) and the quasi-free background of integrated yield (Ex<15MeV) 10 times as much as that of the signal events were assumed.

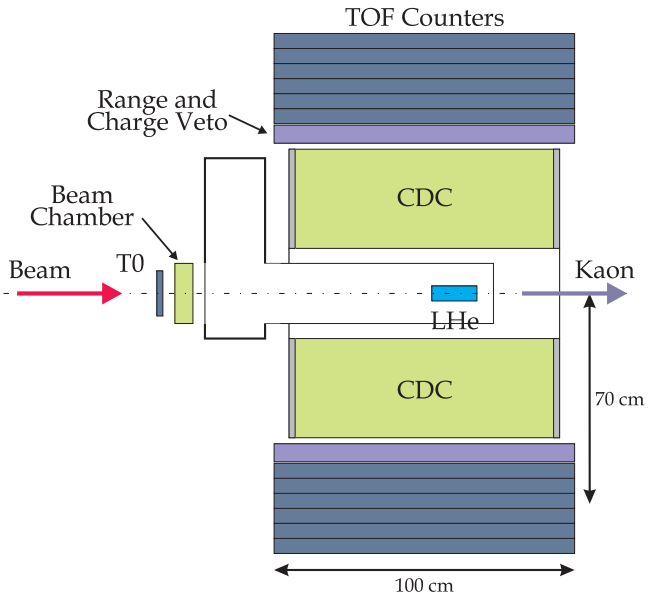

Figure 10: A conceptual design of the decay arm detector system. Figure shows a side view.

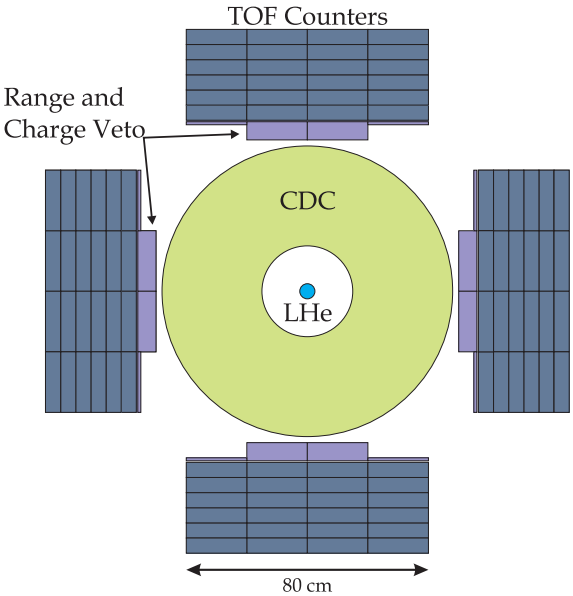

Figure 11: Same as Fig.10. Figure shows a beam view.

Table 4: Current design of the layers of the range counter system and readout methods.

layer	width×length	thickness	readout
1st	200mm×1000mm	10 mm	light guide and conventional PMT
2nd–10th	200mm×1000mm	5 mm	WLS-fiber and multi-anode PMT

built for the J-PARC E15 experiment under a collaboration of RIKEN-KEK-Osaka-OsakaEC, and it will be able to use for this experiment without any modifications. A tracking of π^- is crucial in this experiment because stopping of a negative pion in materials produces several nucleons after the π^- absorption at rest, and the nucleons become a source of background in the NMWD measurement especially for the $\Lambda n \to nn$ process. The rejection of π^- was usually done by more simple detectors, like thin plastic scintillation detectors, in experiments in the past, but additional material around the target due to the detectors became a source of the π^- stopping. We believe CDC is a better solution for the π^- rejection from a view point of the amount of materials around the target. The effects of the π^- absorption at rest to the NMWD measurement is discussed in detail in Sec.3.1.5. CDC helps also the tracking of protons which is necessary to determine the emission angle of the proton relative to the neutron emission.

The range counter system consists of layers of thin plastic scintillation detectors, and are used to identify and determine the energy of charged particles (protons and pions) by measuring the stopping-power, total energy deposit, stopping range and hit position. Table 4 shows current design of the range counter system. The 1st layer of the range counter system is used for the measurement of the stopping-power and hit position, and is read out by ordinary PMT to achieve good timing and energy resolutions. The layers from 2nd to 10th are mainly used for the stopping range determination.

For the neutron detection, layers of thick plastic scintillation detectors (TOF counter system) are used and energies of neutrons are determined by measuring the time-of-flight between the start timing counter in the pion beam (T0) and the TOF modules. Expected overall timing resolution for the time-of-flight measurement is about 200 ps (σ). A typical flight length of particles from the LHe target to the TOF modules is 70cm, and the distance is long enough for a γ/n separation with the 200 ps time resolution: cf., typical $\mathrm{tof}_N - \mathrm{tof}_\gamma = 2$ns. The detection efficiency of energetic neutrons from NMWD is roughly 1%/cm if we set the detector threshold to 1 MeV_{ee}, and we expect about 30% efficiency with the TOF counter system of 30 cm in thickness. In front of the TOF counter system, one layer of 10 mm plastic scintillation detector is placed to veto charged particles (charge veto). The size and design of the charge veto is same as that of the 1st layer of the range counter system.

The size and design of the decay arm modules are almost same with that used in the recent experiments to measure NMWD at KEK-PS (E462, E508, etc.), where we confirmed that the n/γ separation and the kinetic energy measurement could be done well. The acceptance of the decay arm will be improved considerably from that of the previous experiments. Further, the introduction of the range counter system improves the quality of the π/p separation. A range counter system with a similar structure has been used in the KEK-PS-E307 experiment and it had an excellent performance of the π/p separation[50].

3.1.3 Yield estimation in case of the ^{4}He$(\pi^+, K^+)^4_\Lambda$He reaction

Table 5 shows basic parameters to estimate the yield of the NMWD events. The value of the pion beam momentum is set to relatively lower value, 1.1 GeV/c, because the SKS acceptance

Table 5: Basic parameters for the measurement of the ${}^{4}_{\Lambda}$He NMWD events.

Parameters	Values	Parameter in Eqs.(2)–(4)
π^+ beam momentum	1.1 GeV/c	
π^+ beam intensity	1×10^7 /spill	N_{Beam}
PS acceleration cycle	3.4 sec/spill	T_{Cycle}
^{4}He target thickness	2 g/cm^2	N_{Target}
Reaction cross section	10 μb/sr	$d\sigma/d\Omega$
Spectrometer solid angle	0.1 sr	Ω_{SP}
Spectrometer efficiency	0.5	ε_{SP}
Analysis efficiency	0.5	ε_{Anal}
Decay counter acceptance for proton	0.25	a^p_{Decay}
Decay counter acceptance for neutron	0.4	a^n_{Decay}
Efficiency for decay protons	0.8	ε_p
Efficiency for decay neutrons	0.3	ε_n
Branching ratio of $\Lambda n \rightarrow nn$ process	0.01	$BR(\Lambda n \rightarrow nn)$
Branching ratio of $\Lambda p \rightarrow np$ process	0.1*	$BR(\Lambda p \rightarrow np)$

* Experimentally obtained branching ratio is 0.16 ± 0.02 [22, 14].

for the scattered K^+ decreases as the increase of the beam energy and the momentum resolution also gets worse. The rate of the ${}^{4}_{\Lambda}$He(0^+) production is estimated as follows:

$$Yield\ ({}^{4}_{\Lambda}\mathrm{He}(0^+)) = N_{Beam} \times \frac{N_{Target}}{4} \times N_A \times \frac{d\sigma}{d\Omega} \times \Omega_{SP} \times \varepsilon_{SP} \times \varepsilon_{Anal} \times \frac{Time}{T_{Cycle}} \qquad (2)$$

We expect 0.75 ${}^{4}_{\Lambda}$He(0^+)/spill $\sim$ 19k ${}^{4}_{\Lambda}$He(0^+)/day. By using parameters in Table 5, the event rates of the $\Lambda n \rightarrow nn$ and $\Lambda p \rightarrow np$ processes are estimated as follows:

$$Yield\ (\Lambda n \rightarrow nn) = Yield\ ({}^{4}_{\Lambda}\mathrm{He}(0^+)) \times BR(\Lambda n \rightarrow nn) \times (a^n_{Decay} \times \varepsilon_n)^2 \qquad (3)$$

$$Yield\ (\Lambda p \rightarrow pn) = Yield\ ({}^{4}_{\Lambda}\mathrm{He}(0^+)) \times BR(\Lambda n \rightarrow pn) \times (a^n_{Decay} \times \varepsilon_n) \times (a^p_{Decay} \times \varepsilon_p) \qquad (4)$$

We expect 75 events for the $\Lambda n \rightarrow nn$ decay and 1300 events for the $\Lambda p \rightarrow np$ decay in 4 weeks of beam time, and we can achieve 12% statistical error even for the rare $\Lambda n \rightarrow nn$ decay process (if branching ratio is $\sim$1%). Please note that the current $\Gamma(\Lambda n \rightarrow nn)$ is just consistent with zero, $\Gamma(\Lambda n \rightarrow nn) = (0.06^{+0.28}_{-0.06})\Gamma_\Lambda$[22], and a finite value is not obtained, yet. We will be able to set a finite branching ratio of the $\Lambda n \rightarrow nn$ process in the ${}^{4}_{\Lambda}$He hypernucleus in good accuracy for the first time. We believe we will be able to pin down the NMWD amplitudes as we discussed in Sec.2.1.3 and Fig.4.

In the discussion above, we ignored the actual geometry of the decay arm and used averaged acceptances for protons and neutrons, a^p_{Decay} and a^n_{Decay}. The practical detector acceptances are calculated for pn and nn pairs as functions of cos of the pn and nn opening angles by considering the practical geometries of the decay arm, and the results are shown in Figs.12 and 13. The detection efficiencies in the figures should be compared with a^n_{Decay} in Table 5, and the efficiencies in the back-to-back region, $\theta_{pn} < -0.8$ and $\theta_{pn} < -0.8$, are about 1.5 times larger than the averaged value, a^n_{Decay}=0.4. So, we expect slightly larger yields in the measurement of the back-to-back configuration.

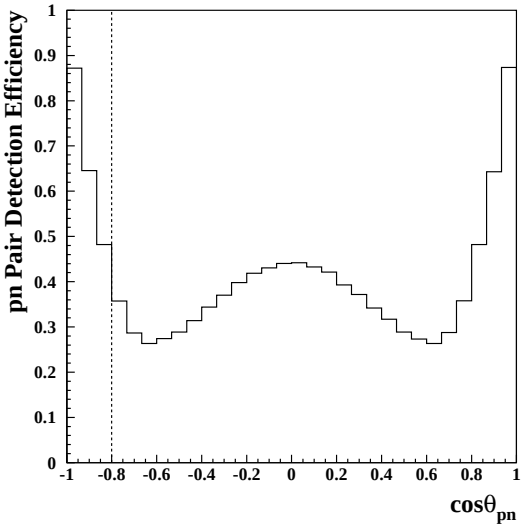

Figure 12: Efficiency of the *pn* pair detection as a function of cos of the *pn* opening angle. The number should be compared with a^n_{Decay} in Table 5.

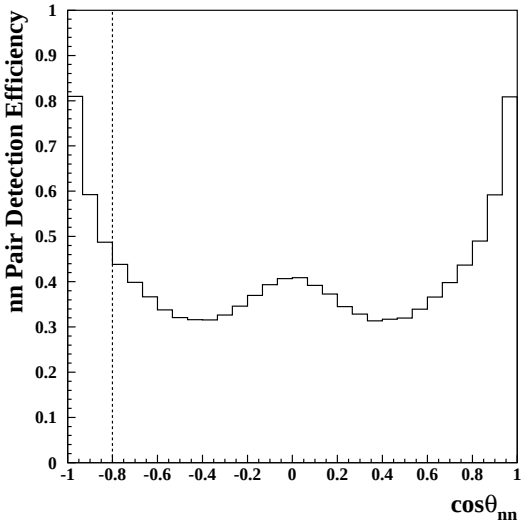

Figure 13: Same plot as Fig.12 for the *nn* pair detection.

Table 6: Basic parameters to estimate the ${}^4_\Lambda$He(0^+) yield by the (K^-, π^-) reaction.

Parameters	Values	Parameter in Eq.(2)
K^- beam momentum	0.90 GeV/c	
K^- beam intensity	3.6×10^5 /spill	N_{Beam}
PS acceleration cycle	3.4 sec/spill	T_{Cycle}
^{4}He target thickness	2 g/cm^2	N_{Target}
Reaction cross section	1.5 mb/sr	$d\sigma/d\Omega$
Spectrometer solid angle	0.02 sr	Ω_{SP}
Spectrometer efficiency	0.8	ε_{SP}
Analysis efficiency	0.5	ε_{Anal}

3.1.4 Possibility of the ^{4}He$(K^-, \pi^-)^4_\Lambda$He reaction

In the previous section, we described an experiment at the K1.8 beamline with intense π^+ beams and SKS. Another option is an experiment with K^- beams at the K1.1 or K1.8BR beamline. The parameters necessary to estimate yields for the case of the (K^-, π^-) reaction are listed in Table 6. The beam intensity estimation assumed the PS operation at 30 GeV, the primary proton beam intensity of 9 μA, and 0.9 GeV/c operation of the beamline. The SPES2 spectrometer was used and the reaction cross section came from the DWIA calculation[42]. Figure 14(a) shows the theoretical differential cross section as a function of the K^- beam momentum. Since the K^- beam intensity at the secondary target strongly depends on the beam momentum due to the short kaon decay distance, the product of the differential cross section and the K^- beam intensity is also plotted in Fig.14(b). The value of the product in (b) for the 0.9 GeV/c beam momentum is not the maximum value (it has the maximum at around 1.1 GeV/c), but the beam momentum is limited by the maximum magnetic rigidity of the SPES2 spectrometer.

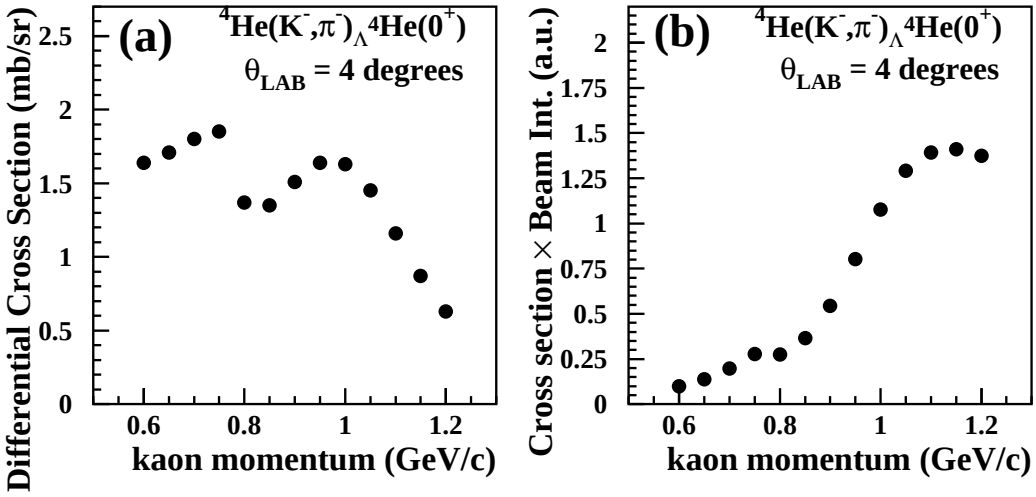

Figure 14: (a) Theoretically estimated differential cross section of the ^{4}He$(K^-,\pi^-)^4_\Lambda$He(g.s., 0^+) reaction at θ_{LAB}=4° based on the DWIA calculation[42], and (b) the product of the differential cross section and the kaon beam intensity at the secondary target.

An event rate estimation resulted in ∼33k $^4_\Lambda$He(0^+)/day. Although the rate is higher than that by the (π^+,K^+) reaction, we think the option of the (K^-,π^-) reaction at the K1.1 or K1.8BR beamline has much larger ambiguity than the experiment at K1.8: e.g., the beamline construction schedule, the K^- beam intensity at the early stage of the 50GeV PS operation, K^- decay backgrounds, etc.

3.1.5 Effects of π^- absorption at rest

Since we will investigate the NMWD of $^4_\Lambda$He hypernuclei and the branching ratio of the $\Lambda n \rightarrow nn$ process is believed to be considerably small (1–4%), some backgrounds of energetic neutron may affect to the precision of the measurement. In the proposed experiment, we will identify the (π^+,K^+) reaction very cleanly and select the $^4_\Lambda$He(g.s.) productions in the ^{4}He(π^+,K^+) reaction by the missing-mass methods with a good mass resolution. So, we believe we can safely remove backgrounds from reactions without hyperon production, such as the (π^+,πnn) reaction. Another candidate of the background is a quasi-free production of a Λ hyperon followed by the $\Lambda \rightarrow \pi^- p$ decay and the π^- absorption at rest because the π^- absorption may produce several energetic nucleons. The background may be reduced considerably again by the missing-mass cut, because the signal region (Λ bound region) is well separated from the quasi-free region (see Fig.9).

We think the most serious background process is the neutron emission of the π^- absorption at rest after the mesonic weak decay (MWD) of the $^4_\Lambda$He hypernucleus:

$$^4_\Lambda\mathrm{He} \;\rightarrow\; ^3\mathrm{He} + p + \pi^-, \qquad \pi^- + A \;\rightarrow\; n + n + X.$$

The background can not be removed by the missing-mass method because it comes from the $^4_\Lambda$He hypernucleus. If the π^- is stopped around the target and the absorption process emits two energetic neutrons, in principle, it is very hard to discriminate the background events from the signal events. The end point of the π^- momentum from the MWD process is estimated to be about 103 MeV/c which corresponds to a stopping-range of roughly 5.5 g/cm^2 in low Z materials. The most thick material around the target is the liquid He target itself in our

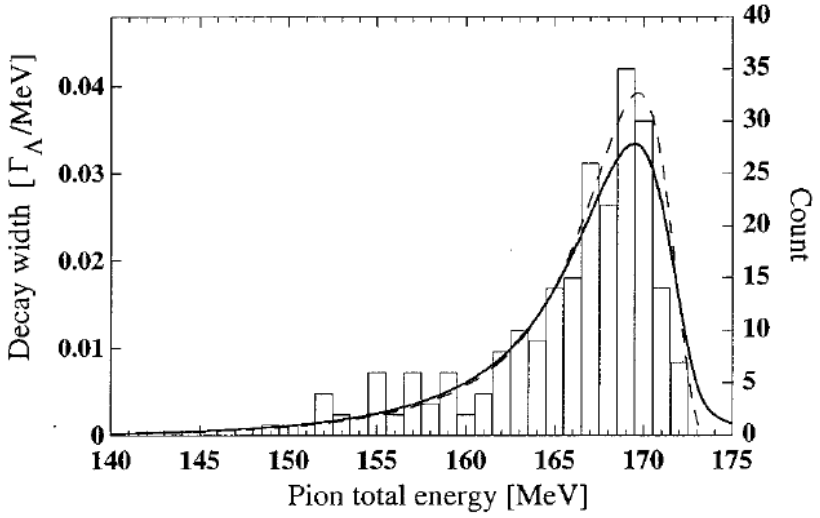

Figure 15: Distribution of π^- total energies from the MWD process of the ${}^{4}_{\Lambda}$He hypernucleus shown in Ref.[51]. The solid line shows a results of a realistic theoretical calculation. The histogram shows a distribution experimentally obtained.

proposed setup, and the maximum thickness is about 2 g/cm^2. So, we believe the major π^-'s from the MWD process do not stop around the target. Some fraction of π^-'s go through CDC and the π^- rejection by CDC works well. Other π^-'s are emitted to the direction close to the beamline, and stop in materials more than 0.5 m away from the target.

Of course, MWD of the ${}^{4}_{\Lambda}$He hypernucleus is a 3-body decay and the momentum of π^- may become considerably small. Figure 15 shows a distribution of π^- total energies from the MWD process of the ${}^{4}_{\Lambda}$He hypernucleus by a realistic theoretical calculation (solid line) together with an experimental distribution (histogram) presented in Ref.[51]. The 2 g/cm^2 material (maximum thickness of the LHe target) stops π^-'s with total energies smaller than 160 MeV, so about 1/5 of π^-'s from MWD are candidates of the stopping in the target. We wish to emphasize that the average traveling length in the LHe target for π^-'s produced in the target is shorter than 2 g/cm^2 and the fraction of the π^- stopping in the target may be smaller than 1/5. Since the branching ratio of the π^- MWD process of ${}^{4}_{\Lambda}$He was estimated to be about 33% [22], we believe the stopping of π^-'s from MWD in the target is smaller than 7% in the worst case. For the measurement of the $\Lambda n \rightarrow nn$ NMWD at the 1% level of the branching ratio, at least a reduction factor of 7 is necessary for the nn pair events from the π^- absorption to keep the S/N ratio larger than 1.

A Monte Carlo simulation calculation based on GEANT4 was performed to estimate the number of energetic nn pairs from the π^- absorption. In the simulation, 2.5M π^-'s were generated and stopped at the center of the decay arm detector system. Several types of materials of the π^- stopping (Li, C, Al and Fe) were tried. Unfortunately, the simulation of the LHe case was not available because the standard GEANT4 could not treat the π^- absorption process in LHe, so we discuss the π^- absorption background by assuming a smooth Z dependence in the following.

Figure 16 shows the distribution of the summation of kinetic energies, $En1$+$En2$, of the background nn pair detected by the left-right or top-bottom pair of the decay arm pair for Li (a), C (b) and Fe (c). The number of total nn pairs in the figure was about 3050, 9100 and 22500 for the Li, C and Fe cases, respectively. The numbers mean the background reduction

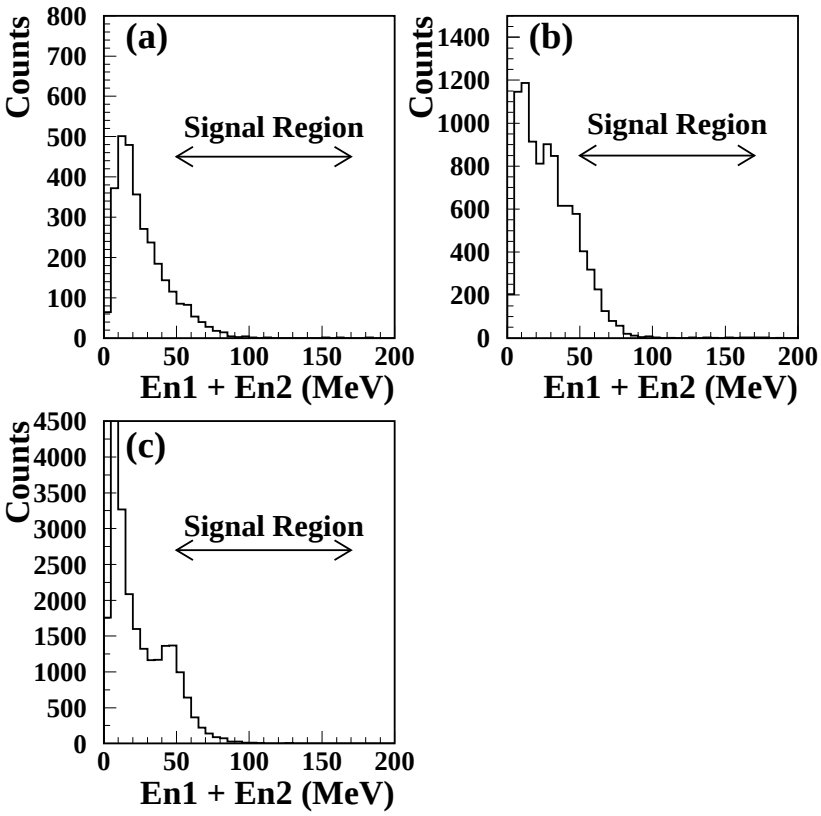

Figure 16: Distribution of the summation of kinetic energies, $En1{+}En2$, of the background nn pair from the π^- absorption detected by the left-right or top-bottom decay arm pair for Li (a), C (b) and Fe (c).

factors by the simple nn pair detection are:

$$3050 \ / \ (2.5\text{M} \times 0.015) = 1/12.2 \qquad \text{for Li}$$

$$9100 \ / \ (2.5\text{M} \times 0.015) = 1/4.1 \qquad \text{for C}$$

$$22500 \ / \ (2.5\text{M} \times 0.015) = 1/1.6 \qquad \text{for Fe}$$

by taking into account about 1.5% of the nn pair detection efficiency with the decay arm. Table 7 shows reduction factors when we make cuts on the sum energy. The amount of the

Table 7: Reduction factors when cuts on the sum energy $En1{+}En2$ are applied.

	reduction factors		
material	50 MeV cut	60 MeV cut	70 MeV cut
Li	1/108	1/227	1/496
C	1/29	1/67	1/177
Fe	1/14	1/35	1/88

reduced background is small enough to achieve a S/N ratio close to 10 even if the stopping material is Fe (the worst case). For the low Z materials, a further reduction of the background

is expected with the same sum energy cut. Since the sum energy of the signal events distribute from 50 to 170 MeV, the inefficiency due to the sum energy cut is not large for the signal events.

4 Time Schedule

Table 8 shows the status of the equipments to be used in the proposed experiment. As shown in the table, the spectrometers (beamline and SKS), liquid He target and CDC will be ready at the Day-1 in collaboration with E05 and E15. For the liquid He target, we will use existing cryostat but need a minor modification of the target He container and the vacuum jacket. The T0 counter and range counter system will be built newly. A half of required number of TOF modules are exist at KEK, and we will built another half of the TOF modules.

Time schedule of the construction of the equipments is shown in Fig.17.

Table 8: Status of the equipments to be used in the proposed experiment.

equipment	status
Beam line spectrometer	to be constructed by E05 Collaboration
SKS	existing at KEK, transfer and upgrade by E05 Collaboration
Liquid He target	existing at RIKEN, need minor modification
T0 detector	new
CDC	to be constructed by E15 Collaboration
Range detector	new
TOF detector	50% existing at KEK, 50% new

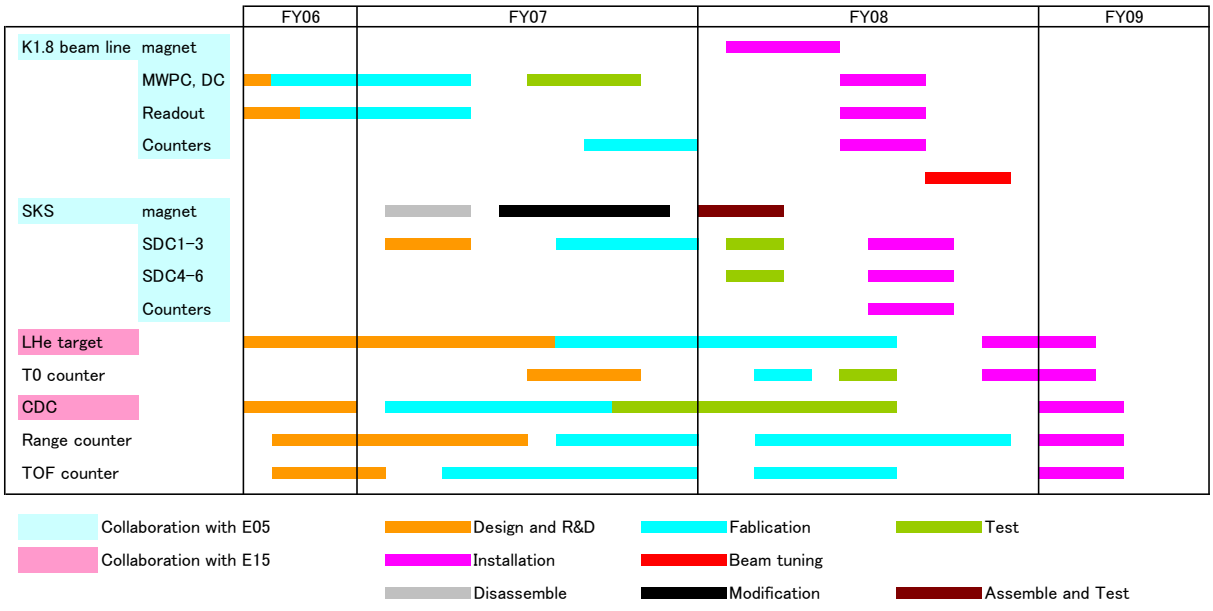

Figure 17: Time schedule of the preparation of each equipment.

5 Cost Estimation

Table 9 shows cost estimation for the equipments to be built or to be modified for the proposed experiment. Most of the equipments will be prepared by the Grant-In-Aid Priority Areas "Multi-quark systems with strangeness" from Japanese Ministry of Education, Culture, Sports, Science and Technology (MEXT). We are planning a recycle use of existing electronics, e.g., HV and discriminators, if possible. We hope a support from J-PARC on some running costs, e.g., LHe and chamber gas.

Table 9: Cost estimation of equipments for the proposed experiment.

equipment	item	cost (JPY)	source
Beam spectrometer	MWPC 1mm	4,000,000	Grant-In-Aid
	MWPC encoder	20,000,000	Grant-In-Aid
liquid He target	modification	2,500,000	Grant-In-Aid
	LHe	3,000,000	
T0 detector	scintillator	500,000	Grant-In-Aid
	PMT	2,000,000	Grant-In-Aid
CDC	mechanical support	1,500,000	Grant-In-Aid
	chamber gas	1,000,000	
Range counter system	scintillator	4,000,000	Grant-In-Aid
	WLS-fiber	500,000	Grant-In-Aid
	multi-anode PMT	3,200,000	Grant-In-Aid
	PMT	1,600,000	Grant-In-Aid
	cable	800,000	Grant-In-Aid
	ADC	1,600,000	Grant-In-Aid
	TDC	1,600,000	Grant-In-Aid
	HV supply		Recycle
	discriminator		Recycle
TOF detector	mechanical support	1,500,000	Grant-In-Aid
	scintillator	7,500,000	Grant-In-Aid
	PMT	12,000,000	Grant-In-Aid
	cable	1,800,000	Grant-In-Aid
	ADC	2,000,000	Grant-In-Aid
	TDC	2,000,000	Grant-In-Aid
	HV supply		Recycle
	discriminator		Recycle

A Measurement of NMWD of ${}^{4}_{\Lambda}$H hypernucleus

As a future experiment, here we describe the study of the NMWD of the ${}^{4}_{\Lambda}$H hypernucleus, although the experiment have to wait the construction of the HIHR beamline. We discuss event rates in the future experiment, but these numbers may have large ambiguity due to the performance of the HIHR beamline and the tolerable maximum count rate of the decay counter system. More realistic estimation can be made after the construction of the HIHR beamline and the studies in the Day-1 experiment.

A.1 Production of ${}^{4}_{\Lambda}$H hypernucleus

To produce ${}^{4}_{\Lambda}$H hypernucleus, we need to use single charge-exchange reactions. Here we propose to use the (π^-, K^0) reaction. Since the ${}^{4}\mathrm{He}(\pi^-, K^0){}^{4}_{\Lambda}\mathrm{H}$ and ${}^{4}\mathrm{He}(\pi^+, K^+){}^{4}_{\Lambda}\mathrm{He}$ reactions are isospin symmetric reactions with each other, we can use the cross section in Fig.6 as an input in the following yield estimation.

The most significant difference between the (π^+, K^+) and the (π^-, K^0) reactions is the detection of the K^0 particle. Since K^0 is usually detected as K_S and K_S decays mainly to a $\pi^+\pi^-$ (68.95%) or $2\pi^0$ (31.05%) pair, the detection efficiency of K^0 is much smaller than that of K^+. To override the difficulty of the small detection efficiency, we propose to use the high-intensity and high-resolution (HIHR) beamline and spectrometer[41]. We can obtain and handle pion beams with intensity up to 10^9 per spill with the HIHR beamline at J-PARC.

The binding energy of the ground state of ${}^{4}_{\Lambda}$H is 2.08 ± 0.06 MeV[44], so the spectrometer have to have a better energy resolution of 1.5 MeV (FWHM). The HIHR beamline and spectrometer system can be designed so that we can have an enough resolution for the study (see Appendix B for more details). Based on the use of the HIHR beamline and experimental parameters listed in Table 10, we estimated the yield of the ${}^{4}_{\Lambda}$H hypernuclei as follows:

Table 10: Basic parameters for the measurement of the ${}^{4}_{\Lambda}$H NMWD events.

Parameters	Values	Parameter in Eqs.(5)
π^+ beam momentum	1.1 GeV/c	
π^+ beam intensity	1×10^9 /spill	N_{Beam}
PS acceleration cycle	3.4 sec/spill	T_{Cycle}
^{4}He target thickness	1 g/cm^2	N_{Target}
Reaction cross section	10 μb/sr	$d\sigma/d\Omega$
Spectrometer solid angle	0.02 sr	Ω_{SP}
Spectrometer efficiency	0.03	ε_{SP}
Analysis efficiency	0.5	ε_{Anal}
Decay counter acceptance for proton	0.26 (or 0.4)	a^p_{Decay}
Decay counter acceptance for neutron	0.4	a^n_{Decay}
Efficiency for decay protons	0.8	ε_p
Efficiency for decay neutrons	0.3	ε_n
Branching ratio of $\Lambda n \to nn$	0.1*	$BR(\Lambda n \to nn)$
Branching ratio of $\Lambda p \to np$	0.01*	$BR(\Lambda p \to np)$

* Experimentally obtained NMWD decay branching ratio, BR($\Lambda n \to nn$)+BR($\Lambda p \to np$), is 0.13 ± 0.08 [22].

$$Yield\ ({}^{4}_{\Lambda}\mathrm{H}) = N_{Beam} \times \frac{N_{Target}}{4} \times N_A \times \frac{d\sigma}{d\Omega} \times \Omega_{SP} \times \varepsilon_{SP} \times \varepsilon_{Anal} \times \frac{Time}{T_{Cycle}} \qquad (5)$$

In Table 10, the spectrometer acceptance ε_{SP} includes the decay branching ratio of K^0 ($K^0 \rightarrow K_S \rightarrow \pi^+\pi^-$; 34.5%) and the efficiency of the detection of the $\pi^+\pi^-$ pair. We expect a production rate of ∼11.4k ${}^{4}_{\Lambda}$H/day.

A.2 Measurement of NMWD

The decay arm detector system discussed in Sec.3.1.2 and shown in Figs.10 and 11 can be used also for this experiment. We expect roughly 460 events for the $\Lambda n \rightarrow nn$ decay and 80 events for $\Lambda p \rightarrow np$ in 4 weeks. We can achieve 11 % statistical error even for the $\Lambda p \rightarrow np$ decay which we have to measure, while we have only the decay rate of the non-mesonic weak decay, $\Gamma_{nm}=(0.17 \pm 0.11)\Gamma_\Lambda$, so far [22]. In the measurement of the ${}^{4}\mathrm{He}(\pi^+, K^+){}^{4}_{\Lambda}\mathrm{He}$ reaction, we have a smaller angular acceptance for the proton detection than that of neutrons, but the acceptance of the proton side is easily increased by an addition of the range counter modules. We expect an improvement of the decay counter acceptance for protons, $a^p_{Decay} = 0.26 \rightarrow 0.4$.

As discussed in Sec.3.1.5, the π^- absorption at rest is a possible background for the measurement of the NMWD process. The π^- partial decay width for ${}^{4}_{\Lambda}$H hypernucleus, $\Gamma_{\pi^-}({}^{4}_{\Lambda}\mathrm{H})=(1.00^{+0.18}_{-0.15})\Gamma_\Lambda$ [20], is roughly 3 times larger than that for the ${}^{4}_{\Lambda}$He hypernucleus, $\Gamma_{\pi^-}({}^{4}_{\Lambda}\mathrm{He})=(0.33 \pm 0.05)\Gamma_\Lambda$ [22]. Fortunately, the π^- absorption background is serious only for the nn pair detection and the branching ratio to the nn channel is expected to be 10% level for the ${}^{4}_{\Lambda}$H hypernucleus (1% level for ${}^{4}_{\Lambda}$He), and the overall S/N ratio is expected to be 3 times better compared with the ${}^{4}_{\Lambda}$He case.

B High-Resolution GeV-Pion Beam line

The main proton synchrotron of J-PARC will deliver a high-power beam of 50 GeV and 15 μA. By taking advantage of the low-emittance primary beam, a *High-Intensity and High-Resolution (HIHR) GeV-Pion Beam Line* can be designed. The beam line will provide a pion intensity as high as 10^9 per second and a momentum resolution as good as 10^{-4}, which are respectively 1000-times more and 10-times better than those realized at K6 of the KEK 12-GeV PS [52]

The present beam-line facility will enable us to increase the production rate of hypernuclei drastically, and will provide us a so-called hypernuclear factory with the (π, K^+) reaction. The (π, K^+) reaction has unique features; 1) it favors to populate stretched states, 2) can produce polarized hypernuclei, and 3) is a background-free reaction. The (π, K^+) reaction plays a complementary role on the hypernuclear study to the (K^-, π) reaction. Thus, the pion beam line should be constructed. Utilizing the present facility, next-generation hypernuclear studies with high precision will be proceeded at J-PARC, where *high resolution, high statistics, and high sensitivity* will be key issues.

A layout of the proposed beam line is illustrated in Fig.18, together with a kaon spectrometer. The beam line consists of two halves. The first half is from PP to MS and for separating

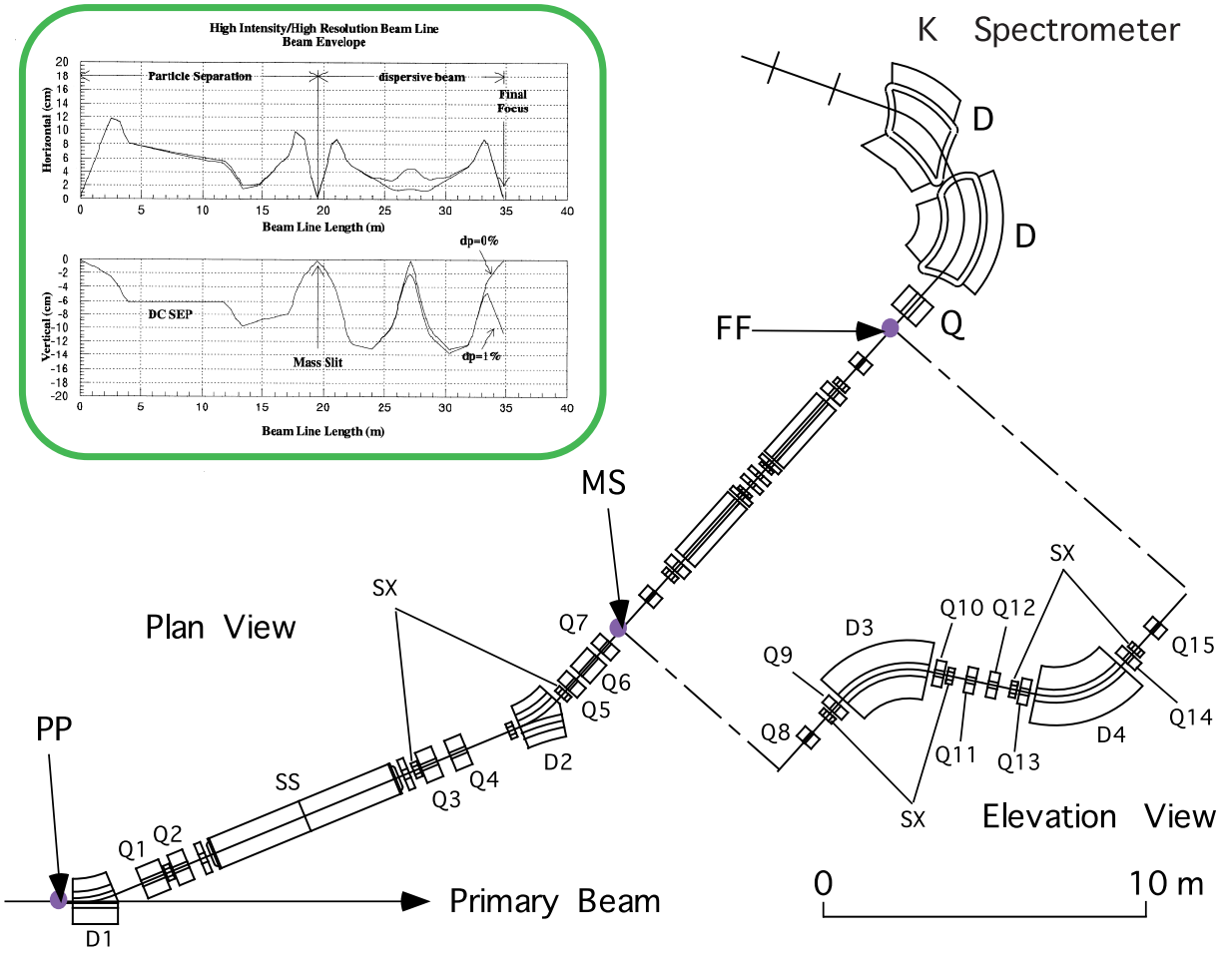

Figure 18: Layout of high-intensity and high-resolution pion beam line and kaon spectrometer.

pions from the other secondary particles with an electrostatic separator. The first part is so called "K1.8-BR" beam-line and will be constructed as the upstream part of the "K1.8" beam-line.

Since no tracking devices are available, due to the high counting rate, the beam momentum must be determined by measuring the reaction point where the beam position is strongly correlated with its momentum. Thus, the second half is from MS to FF and for making the beam dispersive vertically at FF. The dispersion and vertical magnification at FF are to be $\sim$10cm/% and -0.4, respectively. A momentum resolution of 10^{-4} can be achieved when the source size (production target) is smaller than 2.5mm.

The total length and acceptance of the beam line are 35m and 4msr·%. According to the Sanford-Wang formula[53] the π^+intensity is estimated to be more than 10^9 per second with a platinum production target 6cm long.

The kaon spectrometer in the figure is designed to be a resolution as good as 10^{-4} to match with the pion beam line. This is obviously optimized for the resolution, compromising with the acceptance and kaon survival rate. The specifications of the kaon spectrometer should be changed, if necessary, so that the resolution, acceptance, maximum central momentum, total length, cost, and so on, will have to meet experimental requests. The design concept of the kaon spectrometer is summarized as follows.

1. The kaon momentum is determined by the hit position at the focal plane. The resolution is almost determined by the horizontal beam size at the experimental target.

2. The vertical vertex point can be reconstructed from the vertical position and divergence at the focal plane. The vertex resolution of less than 1mm is thus required so that the beam momentum resolution is to be 10^{-4}, which is predominantly determined by the primary beam size at the production target.

3. Satisfying items 1 and 2, we could remove any vertex detectors at around the target, where the counting rate is expected to be too high to drive counters.

We could design a kaon spectrometer to meet above conditions. The horizontal magnification and dispersion are -0.851 and 8.327 cm/%, respectively. The vertical magnification ($R33$) is -3.08. Since the spectrometer has a vertical focus, the vertex resolution is determined by Y_O=$Y_I/R33 \sim$ 0.5mm/3.08 $\sim$ 0.16mm $<<$ 1mm, where Y_O and Y_I represent the vertex resolution (object size) and position resolution (image size) at the focal plane, respectively.

Specifications of the pion beam line and kaon spectrometer are summarized in Table 11.

Table 11: Specifications of the pion beam line and kaon spectrometer.

	π Beam Line	K Spectrometer
Max. Central Momentum (GeV/c)	1.5	1.5
Total Length (m)	34.738	12.4
Horizontal Acceptance (mrad)	$\pm$50	$\pm$100
Vertical Acceptance (mrad)	$\pm$10	$\pm$40
Momentum acceptance (%)	$\pm$1	$\pm$5
Horizontal Magnification	0.773	-0.851
Vertical Magnification	-0.409	-3.084
Dispersion (cm/%)	10.614	8.327
Momentum Resolution ($\Delta P/P$)	10^{-4}	10^{-4} [a)]

[a)] Corrections for higher order aberrations are required.

An updated layout of the high-intensity and high-resolution beamline and kaon spectrometer fitted to current floor plan of the experimental hall is shown in Fig.19.

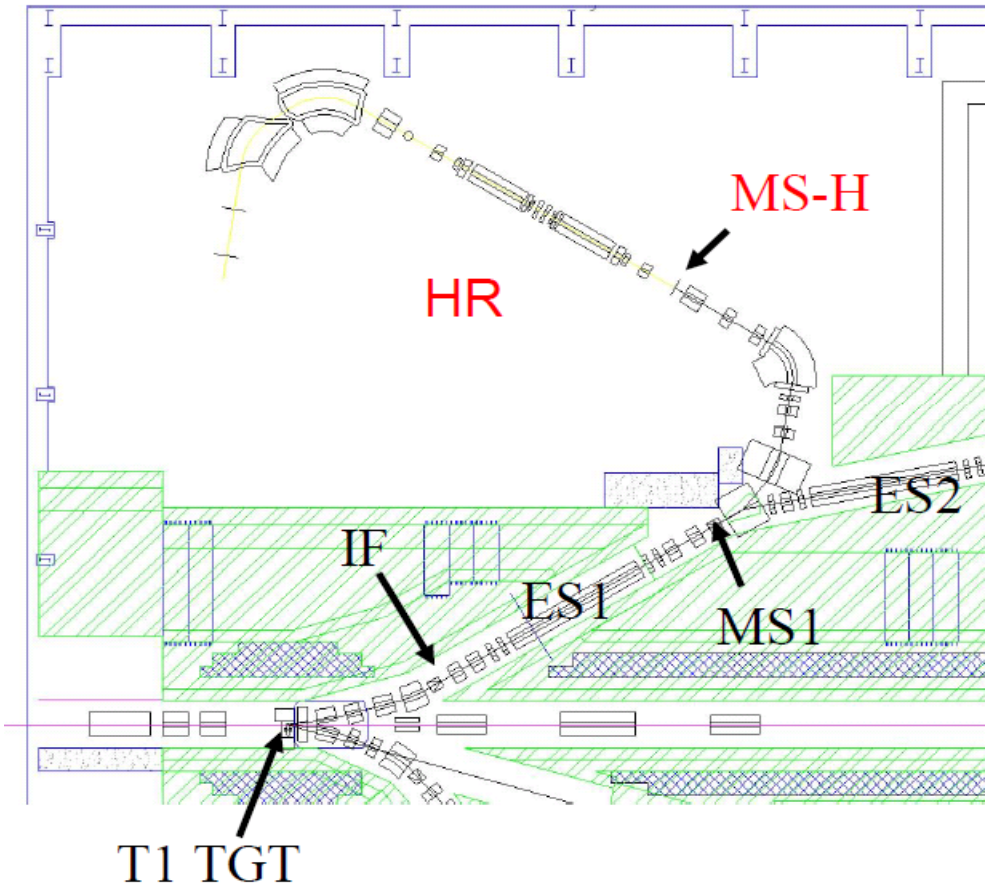

Figure 19: Layout of high-intensity and high-resolution pion beam line fitted to the current floor plan of the experimental hall.

References

[1] M. Danysz and J. Pniewski, Bull. Acad. Pol. Sci. III **1** (1953) 42; M. Danysz and J. Pniewski, Phil. Mag. **44** (1953) 348.

[2] T. Inoue, S. Takeuchi and M. Oka, Nucl. Phys. **A577** (1994) 281c; Nucl. Phys. **A597** (1996) 563.

[3] M.M. Block and R.H. Dalitz, Phys. Rev. Lett. **11** (1963) 96.

[4] J.J. Szymanski, *et al.*, Phys. Rev. **C43** (1991) 849.

[5] H. Noumi, *et al.*, Phys. Rev. **C52** (1995) 2936.

[6] B.H.J. McKellar and B.F. Gibson, Phys. Rev. **C30** (1984) 322.

[7] K. Takeuchi, H. Takaki and H. Bando, Prog. Theor. Phys. **73** (1985) 841.

[8] J. Dubach, Nucl. Phys. **A450** (1986) 71c.

[9] A. Parreño, A. Ramos, and C. Bennhold, Phys. Rev. **C56** (1997) 339, and references therein.

[10] H. Outa, *et al.*, KEK-PS E462 proposal.

[11] H. Bhang, *et al.*, KEK-PS E508 proposal.

[12] Shoji Shinmura, Prog. Theor. Phys. **97** (1997) 283.

[13] A. Ramos, M.J. Vicente-Vacas and E. Oset, Phys. Rev. **C55** (1997) 735.

[14] V.J. Zeps, Nucl. Phys. **A639** (1998) 261c.

[15] B.H. Kang, *et al.*, Phys. Rev. Lett. **96** (2006) 062301.

[16] H. Outa, *et al.*, Nucl. Phys. **A754** (2005) 157c.

[17] M.J. Kim, *et al.*, nucl-ex/0601029 (2006).

[18] H.G. Miller, M.W. Holland, J.P. Roalsvig and R.G. Sorensen, Phys. Rev. **167** (1968) 922.

[19] I.R. Kenyon, A.Z.M. Ismail, A.W. Key, S. Lokanathan and Y. Prakash, Nuovo Cimento **30** (1963) 1365.

[20] M.M. Block, *et al.*, Proceedings of the International Conference on Hyperfragments, St. Cergue, 1963 [CERN Report No. 64-1, 1964].

[21] N.K. Rao and M.S. Swami, Proc. Indian Acad. Sci. **71A** (1970) 100.

[22] H. Outa, *et al.*, Nucl. Phys. **A639** (1998) 251c.

[23] A. Parreño and A. Ramos, Phys. Rev. **C65** (2001) 015204.

[24] Kenji Sasaki, Takashi Inoue and Makoto Oka, Nucl. Phys. **A669** (2000) 331; Nucl. Phys. **A678** (2000) 455.

[25] Kazunori Itonaga, Toshio Motoba and Tamotsu Ueda, Mod. Phys. Lett. **A18** (2003) 135.

[26] T. Kishimoto, KEK-Report No. 83-6 (1983) 51, unpublished.

[27] H. Nabetani, T. Ogaito, T. Sato and T. Kishimoto, Phys. Rev. **C60** (1999) 017001.

[28] H. Bando, T. Motoba and J. Zofka, Int. J. Mod. Phys. **5** (1990) 4021.

[29] K. Sasaki, T. Inoue and M. Oka, Nucl. Phys. **A707** (2002) 477.

[30] S. Ajimura, *et al.*, Phys. Lett. **B282** (1992) 293.

[31] T. Kishimoto, *et al.*, KEK-PS E278 proposal.

[32] S. Ajimura, *et al.*, Phys. Rev. Lett. **80** (1998) 3471.

[33] K. Itonaga, T. Motoba, O. Richter and M. Sotona, Phys. Rev. **C49** (1994) 1045.

[34] S. Ajimura, *et al.*, Phys. Rev. Lett. **84** (2000) 4052.

[35] C. Bennhold and A. Ramos, Phys. Rev. **C45** (1992) 3017.

[36] T. Maruta, *et al.*, nucl-ex/0509016 (2005); H. Outa, private communication, 2006.

[37] K. Sasaki, M. Izaki and M. Oka, Phys. Rev. **C71** (2005) 035502.

[38] K. Itonaga, private communication, 2006.

[39] Since the theoretical calculation in Ref. [37] introduced strong violation of the ΔI=1/2 rule, it was not adequate to plot the result directly in Fig.3. We used their predictions on the NMWD rates to compare with the model independent analysis.

[40] R.A. Schumacher, Nucl. Phys. **A547** (1992) 143c.

[41] H. Noumi, Nucl. Phys. **A639** (1998) 121c.

[42] T. Harada, private communication, 2006.

[43] There are two magnetic spectrometers available at Day-1 in the J-PARC 50 GeV PS facility. One is the Superconducting Kaon Spectrometer (SKS) that has a large acceptance ($\sim$100 msr) and a good momentum resolution ($\sim$0.1 %) up to 1.2 GeV/c for the (π^+, K^+) reaction. An upgrade of the SKS spectrometer is planning to accept more higher beam momentum (SksPlus) but the update reduces the acceptance considerably ($\sim$25 msr). Another spectrometer is SPES2 that has an acceptance of 20 msr up to 1.1 GeV/c.

[44] M. Juric, *et al.*, Nucl. Phys. **B52** (1973) 1.

[45] T. Hasegawa, *et al.*, Phys. Rev. **C53** (1996) 1210.

[46] H. Hotchi, *et al.*, Phys. Rev. **C64** (2001) 044302.

[47] J.H. Kim, *et al.*, Phys. Rev. **C68** (2003) 0605201.

[48] J. Sasao, *et al.*, Phys. Lett. **B579** (2004) 258.

[49] P.K. Saha, *et al.*, Phys. Rev. Lett. **94** (2005) 052502.

[50] Y. Sato, *et al.*, Nucl. Phys. **A691** (2001) 189c.

[51] Izumi Kumagai-Fuse, Shigeto Okabe and Yoshinori Akaishi, Phys. Rev. **C54** (1996) 2843.

[52] The K6-SKS spectrometer system has realized about 50 events of the ${}^{12}_{\Lambda}$C production per hour with a graphite target 1.8g/cm^2 thick.

[53] J.R. Sanford and C.L. Wang, BNL 11279 and BNL 11479 (1967); C.L. Wang, Phys. Rev. Lett. **25** (1970) 1068.